Journal of Experimental and Theoretical Physics, Vol. 94, No. 5, 2002, pp. 977–984.
Translated from Zhurnal Éksperimental'noĭ i Teoreticheskoĭ Fiziki, Vol. 121, No. 5, 2002, pp. 1139–1148.

SOLIDS
Structure

Lattice Dynamics and Hydrostatic-Pressure-Induced Phase Transitions in ScF_3

K. S. Aleksandrov[a], V. N. Voronov[a], A. N. Vtyurin[b], S. V. Goryainov[b], N. G. Zamkova[a], V. I. Zinenko[a, *], and A. S. Krylov[a]

[a] *Kirenskiĭ Institute of Physics, Siberian Division, Russian Academy of Sciences, Akademgorodok, Krasnoyarsk, 660036 Russia*

[b] *Joint Institute of Geology, Geophysics, and Mineralogy, Siberian Division, Russian Academy of Sciences, Novosibirsk, 630090 Russia*

**e-mail: zvi@iph.krasn.ru*

Received November 13, 2001

Abstract—New phase transitions induced by hydrostatic pressure in a cubic (under standard conditions) ScF_3 crystal are discovered by the methods of polarization microscopy and Raman scattering. The space groups $R\bar{3}c$ for $Z = 2$ and *Pnma* for $Z = 4$ are proposed for the high-pressure phases. A nonempirical computation of the lattice dynamics of the crystal is carried out. It is shown that, under normal pressure, the cubic phase is stable down to $T = 0$ K, while the application of a hydrostatic pressure gives rise to a phonon branch in the vibrational spectrum (between points *R* and *M* of the Brillouin zone) with negative values of squares of frequencies. The condensation of soft mode R_5 at the boundary point of the Brillouin zone leads to rhombohedral distortion of the cubic structure with the unit cell volume doubling. The calculated frequencies at $q = 0$ of the ScF_3 lattice in the distorted rhombohedral phase are real-valued; the number and position of frequencies active in Raman scattering are in accord with the experimental values. © *2002 MAIK "Nauka/Interperiodica".*

1. INTRODUCTION

Fluorides of trivalent metals MeF_3 with an ideal or distorted structure of α-ReO_3 belong to the family of perovskite-like compounds with the general formula ABX_3, in which one of the cation sites is vacant (Fig. 1). Like all perovskites, these substances experience consecutive phase transformations under external effects. The presence of bulk cavities in the structure makes it possible to modify the physical properties of these crystals smoothly by creating structural disorder or by introducing impurities, which makes these crystals interesting objects for studying the mechanisms of phase transitions (see, for example, [1]) and also makes it possible to find their practical applications [2, 3].

Among other compounds with the chemical formula MeF_3, scandium fluoride is apparently the least studied. The most comprehensive reviews devoted to the description of structural phase transitions in perovskites [4, 5] contain no information on this material. In the structural database [6], information is given on three different structures (cubic, rhombohedral, and orthorhombic) of ScF_3 under normal conditions; however, special stability tests of these phases [7] revealed that the orthorhombic phase under normal conditions is metastable, while the cubic phase was not detected at all.

It was noted in [5, 8, 9] that the phase diagram of these crystals is very sensitive to structural defects and impurities, which creates additional difficulties in their investigations. In addition, at least some of the phase transitions in crystals belonging to this family are ferroelastic [1, 4], and the presence of growth stresses in the samples synthesized at high temperatures may also considerably affect their behavior upon a change in external conditions.

In our earlier publication [10], we analyzed the vibrational spectrum of the lattice for the cubic modification of ScF_3 at low temperatures down to 4 K, but no phase transitions were detected. The present work aims at studying phase transitions in a ScF_3 crystal under pressure by using Raman spectroscopy combined with

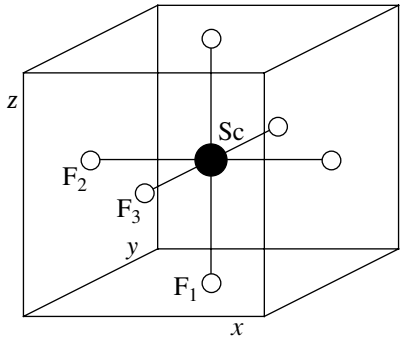

Fig. 1. Structure of the cubic phase of ScF_3.

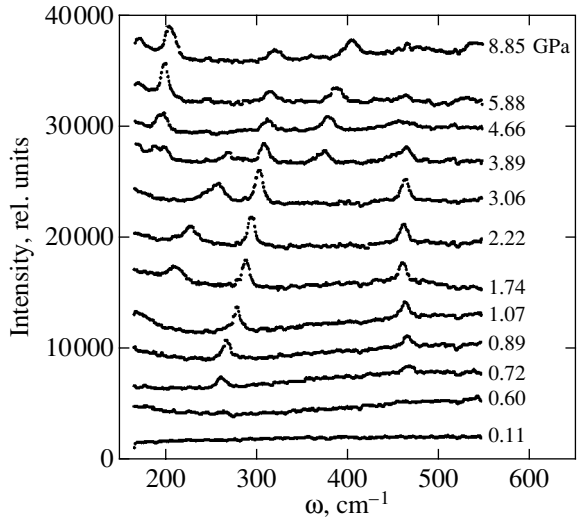

Fig. 2. Variation of the Raman spectrum of ScF_3 upon an increase in pressure.

polarization microscopy on samples synthesized under the conditions ensuring minimal stresses during their growth and at establishing the origin of the lattice instability appearing in this case by using nonempirical calculations of the frequency spectrum of lattice vibrations in the framework of a microscopic model of an ionic crystal.

2. SYNTHESIS AND STRUCTURE OF SINGLE CRYSTALS

We could not find in the literature any technique for growing ScF_3 single crystals; however, the synthesis of similar single crystals of iron and aluminum fluorides from flux in melt is described in [11–13]. It should be noted that this method makes it possible to lower the synthesis temperature and, hence, to reduce the probability of emergence of stresses during the crystal growth. We used lithium fluoride as the solvent. Attempts were made to use other compounds, but the single crystals grown in this case were too small (less than 1 mm^3).

The flux–melt containing 40 mol % ScF_3 was hermetically sealed in an oxygen-free atmosphere in a platinum ampule with a wall thickness of 0.2 mm. Over a period of 14 days, the ampule was lowered at a rate of 20 mm/day in a vertical tube furnace with an axial temperature gradient of 10–20 K/cm from the temperature region of 1400 K.

After cooling and opening the ampule, we discovered a cylindrical sample in it. The lower transparent part of the sample having a diameter of 10 mm and a height of 7 mm did not contain any defects or inclusions that could be seen in the microscope. The X-ray structural analysis proved the correspondence of the obtained crystal to the structure of the cubic phase of ScF_3 with the unit cell parameter $a_0 = 4.01$ Å (a comparison was made against the data presented in [6]). The observation in a polarization microscope revealed the optical isotropy of the crystal, which is also in accord with the cubic symmetry.

3. VARIATION OF RAMAN SPECTRA

The vibrational representation of the space group $Pm\bar{3}m$ of the cubic phase for the center of the Brillouin zone has the form

$$\Gamma_0 = F_{2u} + 3F_{1u}, \quad (1)$$

all vibration being inactive in the Raman spectrum.

A similar expansion for the rhombohedral structure has the form

$$\Gamma_1 = \mathbf{A}_{1g} + 2A_{2g} + 3\mathbf{E}_g + 2A_{1u} + 3A_{2u} + 5E_u, \quad (2)$$

while, for the orthorhombic structure, we have

$$\Gamma_1 = 7\mathbf{A}_g + 5\mathbf{B}_{1g} + 7\mathbf{B}_{2g} + 5\mathbf{B}_{3g} + 5A_u + 7B_{1u} + 5B_{2u} + 7B_{3u}. \quad (3)$$

In expansions (2) and (3), the active modes in the Raman spectrum are singled out.

A comparison of expressions (1)–(3) shows that the selection rules for these structures differ considerably and, hence, these structures should be easily diagnosed from the form of their Raman spectra.

We studied ScF_3 samples under a high (up to 9 GPa) hydrostatic pressure at room temperature on a setup with diamond anvils, which is similar to that used in [14, 15]; the diameter of the cell containing the sample was 0.25 mm, and its height was 0.1 mm. The pressure was determined to within 0.05 GPa from the shift in the luminescence band of a ruby microcrystal [15, 16] placed next to the sample. Mixtures of ethyl and methyl alcohols or glycerene were used as the pressure-transmitting medium. The Raman spectra were generated by radiation emitted by an Ar^+ laser (514.5 nm, 0.5 W) and were recorded by a multichannel spectrometer OMARS 89 (Dilor). In view of the small size of the sample and strong diffuse scattering, the high-frequency (150–600 cm^{-1}) region of the spectrum was recorded. The domain structure and birefringence effects in the sample were observed simultaneously with the help of a polarization microscope.

Under the normal pressure, the crystal has no Raman spectrum; it is optically isotropic and is darkened in crossed polarizers (slight field blooming emerges due to anisotropic mechanical stresses appearing in diamond anvils). Under a pressure of 0.7 GPa, the spectrum acquires two spectral lines (at 260 and 465 cm^{-1}; see Fig. 2), simultaneously, the sample placed between two crossed polarizers is bleached (Fig. 3), indicating the emergence of optical anisotropy. Some samples exhibit splitting into coarse domains (of the

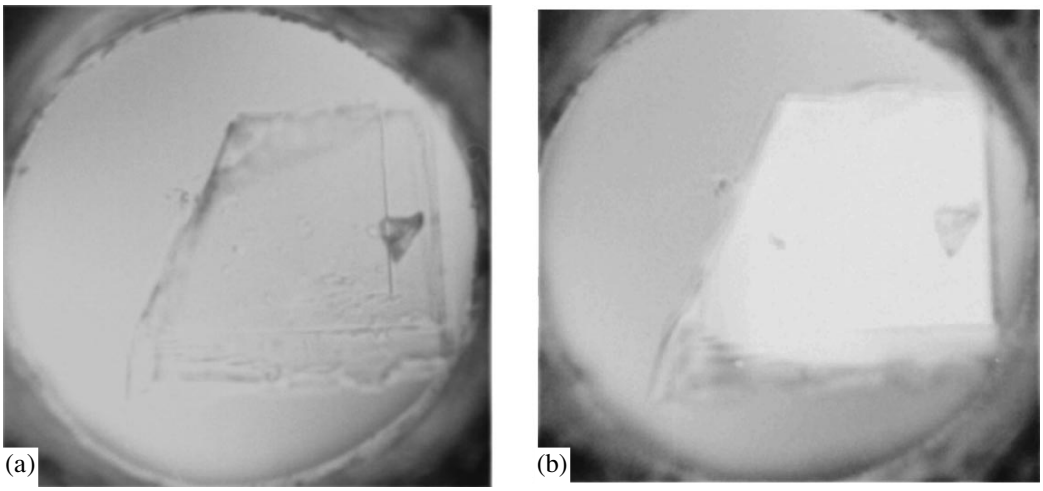

Fig. 3. Microphotographs of a sample before (left, 0.07 GPa) and after (right, 0.72 GPa) the first phase transition. The polarizers of the microscope are crossed. The cell diameter is 0.25 mm.

order of 0.02–0.05 mm) of irregular shape. Upon a further increase in pressure, the intensity of these lines increases monotonically. The frequency of the 260-cm^{-1} line also increases, attaining a value of 300 cm^{-1} under a pressure of 3.8 GPa. In the low-frequency region, one more line appears, shifting monotonically from 180 cm^{-1} at 1.4 GPa to 260 cm^{-1} at 3.8 GPa. This is accompanied by an enhancement of the birefringence effect and a change in the interference coloring of the sample associated with a change in the shape of the optical indicatrix.

The changes occurring up to values of 3.8 GPa are reversible and can be reproduced in different samples taken from the same product of crystallization and with different pressure-transmitting liquids (Fig. 4). Within the experimental error indicated above, no hysteresis effects are observed. The form of the domain structure determined to a considerable extent by defects at the sample boundaries changes from sample to sample and as afunction of the pressure variation rate; the monodomain state can be obtained in well-faceted microcrystals subjected to a slowly increasing pressure.

A further increase in pressure leads to one more transition (at 3.8 GPa). The crystal acquires a complex system of a large number of small (less than 0.01 mm) domains which can be seen through a microscope. The boundaries of these domains strongly scatter light (Fig. 5). Simultaneously, the form of the Raman spectrum changes sharply: some lines disappear, and a considerable number of new lines and bands consisting apparently of a several closely spaced profiles are formed (see Figs. 3 and 4). It should be noted that the pressure of 3.8 GPa corresponding to the transition point is in accord with the pressure of transition from the rhombohedral to the orthorhombic phase of the crystal under investigation, which was observed earlier in [8, 9]. Under a further increase in pressure, the high-frequency (> 200 cm^{-1}) part of the spectrum changes insignificantly, while, below 200 cm^{-1}, a shift of one of the lines towards higher frequencies, its intersection with another line, and, probably, the emergence of one more line in the vicinity of 160 cm^{-1} under a pressure of 7 GPa are observed. The system of domain walls emerging during the transition is slightly modified upon an increase in pressure; the total number of domains slightly decreases, but the system does not disappear completely. The crystal remains optically anisotropic, although strong scattering at domain walls complicates the observation of the effects associated with it.

A decrease in the pressure on a sample in this phase does not lead to a reverse transition (Fig. 6). The system of domain walls and the general nature of the spectrum are preserved, although the spectrum displays the softening of at least one vibration in the low-frequency

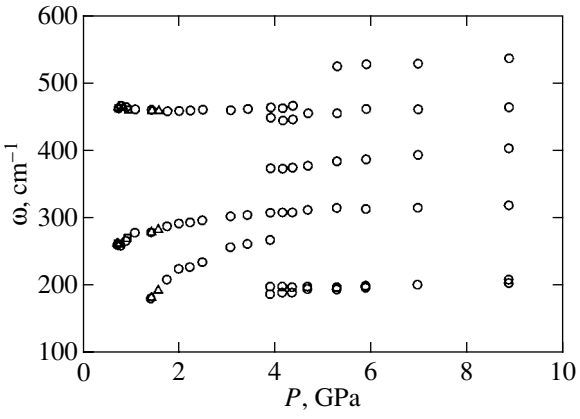

Fig. 4. Pressure dependences of the frequencies of experimentally observed lines. Circles correspond to values obtained under increasing pressure, while squares and triangles correspond to values obtained on different samples in the second phase under decreasing pressure.

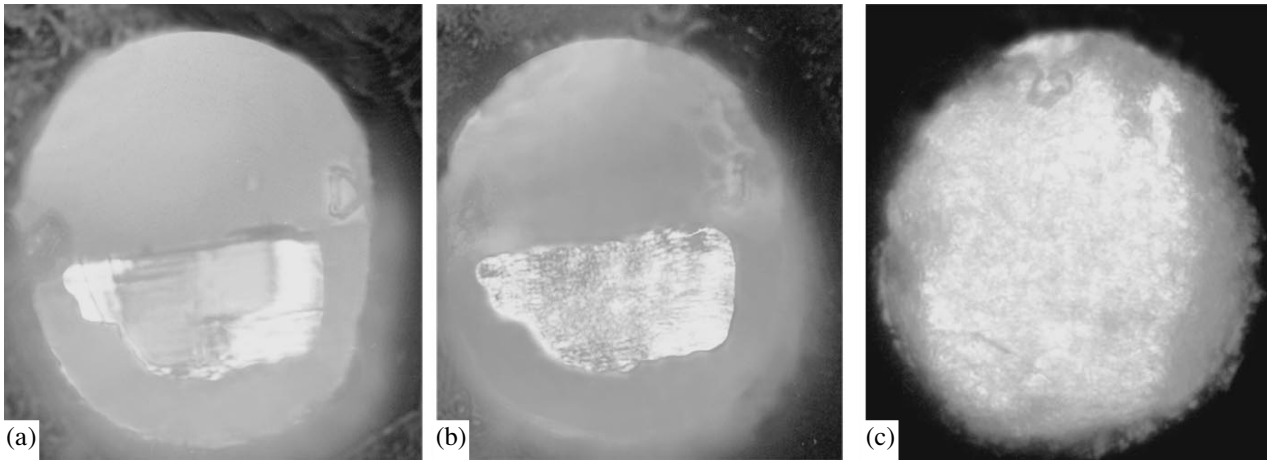

Fig. 5. Microphotographs of a sample before (a, 3.06 GPa) and after (b, 3.89 GPa) second phase transition and after its fracture upon a rapid decrease in pressure (c, 0.1 GPa).

part, which may be due to the emergence of lattice instability. Under a slow (over several hours) decrease in pressure from 1 GPa down to normal pressure, the sample can be preserved (the lower spectrum in Fig. 6 was measured in air on the sample extracted from the cell). A more rapid decrease in pressure below 1 GPa leads to crystal breakdown (see Fig. 5c), indicating the presence of strong mechanical stresses in the sample.

4. LATTICE DYNAMICS

In order to calculate the vibrational spectrum of the ScF_3 crystal lattice, we used a nonempirical model of an ionic crystal, generalizing the Gordon–Kim approximation by taking into account the effect of crystal lattice on the deformability and polarizability of ions [17]. The expression for the dynamic matrix was given in [18]. In the framework of this model, the lattice dynamics of AlF_3, GaF_3, and InF_3 crystals in the cubic phase, which are isomorphic to ScF_3, was calculated earlier and it was shown that the vibration spectrum of these crystals does not contain imaginary frequencies, which indicates the stability of the cubic phase [8].

The equilibrium value of the lattice parameter of the ScF_3 crystal was determined from the minimum of the total energy of the crystal as a function of volume. Table 1 contains this value together with the experimental value as well as the calculated values of polarizabilities of scandium and fluorine ions, high-frequency permittivity ε_∞, and Born dynamic charges. It can be seen that the calculated unit cell parameter is 5% smaller than the experimental value. Unfortunately, the experimental value of ε_∞ for this crystal is unknown, but the obtained value is typical of perovskites contain-

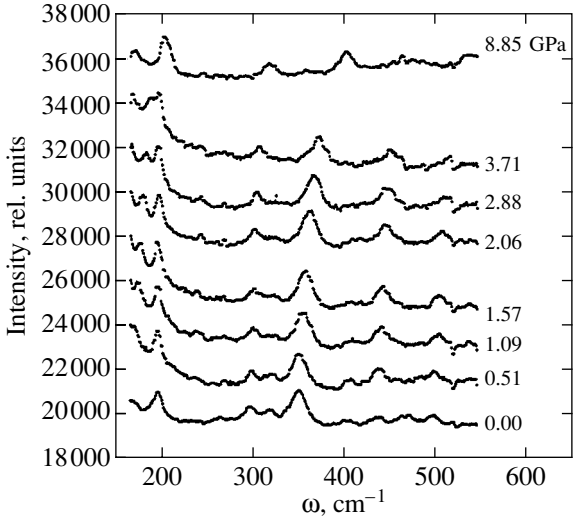

Fig. 6. Variation of the Raman spectrum of ScF_3 upon a decrease in pressure.

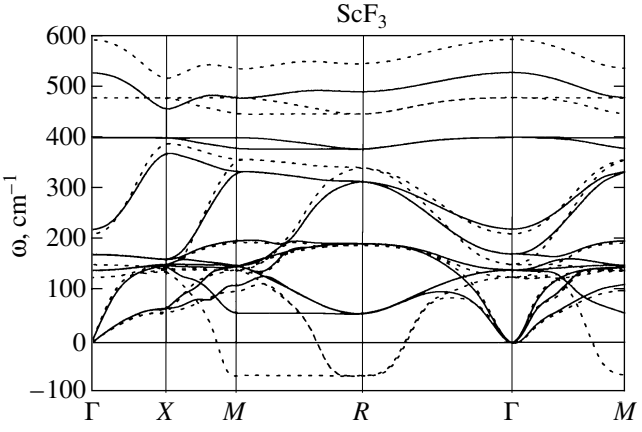

Fig. 7. Results of calculation of the phonon spectrum of the cubic phase of ScF_3. Solid curves correspond to the unit cell parameter a = 7.22 at. units (normal pressure) and dashed curves correspond to a = 7.06 at. units.

ing fluorine. The effective charge tensor for the Sc ion is isotropic in accordance with the symmetry of the position of this ion in the cubic phase, and its value is close to the nominal value of the ion charge (+3). For a fluorine ion, there are two tensor components corresponding to the displacement of the F ion parallel ($Z^*_{\parallel,F}$) and perpendicular ($Z^*_{\perp,F}$) to the Sc–F bond.

The calculated spectrum of ScF_3 lattice vibrations in the cubic phase is shown in Fig. 7 for a unit cell volume of 52.1 Å^3 (corresponding to the applied pressure $P \approx$ 6 GPa). The vibrational spectrum contains no imaginary frequencies (which explains the structural stability down to temperatures of 4 K). However, it contains a weak dispersion branch (between points R and M in the Brillouin zone) with an anomalously low frequency. In this vibrational branch, the triply degenerate mode R_5 at point R and nondegenerate modes in the $R \longrightarrow M$ direction (including point M) correspond to vibrations in which fluorine ions are displaced [19]. The structural phase transitions in most halogenides with the perovskite structure [4], including MeF_3 crystals (Me = Al, Ga, In, …), are associated precisely with the mode condensation of this vibrational branch [1, 2].

We also calculated the vibrational spectrum of the cubic phase of the ScF_3 lattice for nonequilibrium decreasing values of the unit cell parameter, which corresponds to the application of a hydrostatic pressure to the crystal. The value of pressure was estimated from the numerical differentiation of the total energy of the crystal with respect to the volume and from the calculated bulk compression modulus $B = (C_{11} + 2C_{12})/3$ in terms of elastic constants whose values were obtained from the dispersion dependence of acoustic vibrational branches for $\mathbf{q} \longrightarrow 0$ (which are given in Table 1). The curve corresponding to the equation of state of ScF_3 is shown in Fig. 8.

Figure 7 shows that the most significant changes in the lattice vibrational spectrum upon the application of a hydrostatic pressure to the crystal occur in the regions of high and low frequencies of optical vibrational modes. The high-frequency vibrational modes become "harder" upon a decrease in volume, while the branch of lattice vibrations (between points R and M of the Brillouin zone) with anomalously low values of frequency becomes "softer" upon the application of pressure, and the cubic structure of the crystal becomes unstable.

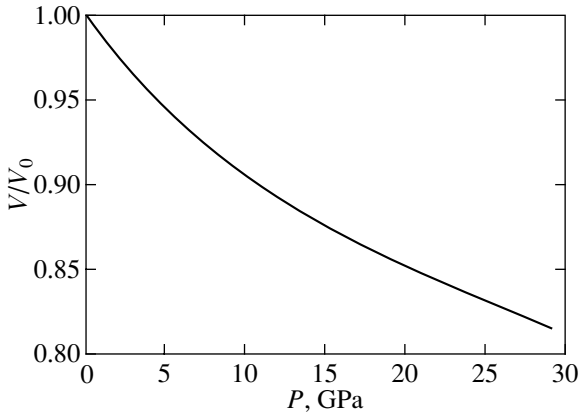

Fig. 8. Calculated equation of state of ScF_3.

5. DISCUSSION

The results of our calculations show that, in accordance with the available experimental data [10], the cubic phase of the ScF_3 crystal under normal pressure remains stable down to $T = 0$ K. At the same time, according to the results of our experiments and an analysis of lattice dynamics, the application of a hydrostatic pressure leads to cubic phase instability. The calculations of the frequencies of lattice vibrations under the action of a hydrostatic pressure show that the softest mode is the triply degenerate mode R_5 belonging to the boundary point $R = \pi/a(1, 1, 1)$ of the Brullouin zone of the cubic phase. Consequently, it is natural to assume that the phase transition observed under a pressure equal to 0.7 GPa is associated with the condensation of precisely this mode.

The solid lines in Fig. 9 show the volume dependence of the squared frequency $\omega^2(R_5)$ of this mode. A decrease in the unit cell volume (increase of pressure) leads to a linear decrease in the value of $\omega^2(R_5)$, so that $\omega^2(R_5) = 0$ for $P \approx 2.5$ GPa (see Fig. 9). The lower experimental value of pressure corresponding to the transition may be due to nonideality of the samples used in experiments; according to [8], structural defects lead to instability of the cubic phase.

A displacement of fluorine ions in the triply degenerate R_5 mode corresponds to the "rotation" of the octahedron ScF_6 [19] about the spatial diagonal of the cubic unit cell. The irreducible representation R_5 appears in the vibrational representation of the crystal only once; consequently, the expression for $\omega^2(R_5)$ in terms of the

Table 1. Results of calculations of the main physical parameters of the cubic phase of ScF_3

a_0, Å, experiment	a_0, Å, theory	Z^*_{Sc}	$Z^*_{\parallel F}$	$Z^*_{\perp F}$	α_{Sc}, Å^3	α_F, Å^3	ε_∞	C_{11}, GPa	C_{12}, GPa	C_{44}, GPa	B, GPa
4.01	3.82	3.36	–0.71	–1.95	0.27	0.72	1.75	172.7	18.9	18.6	70.2

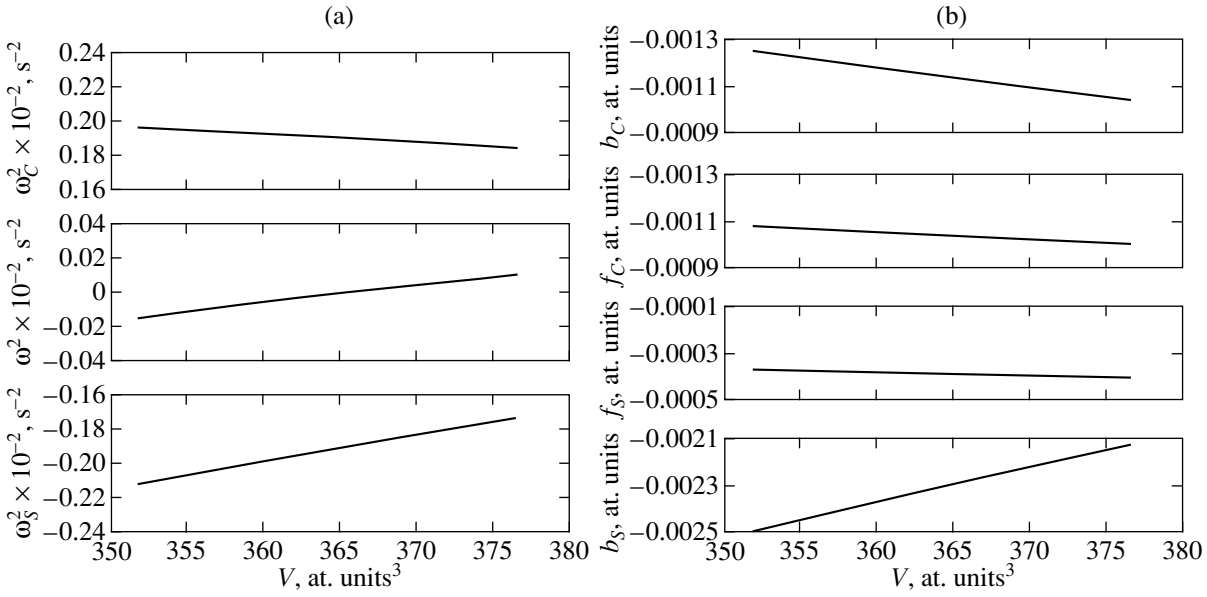

Fig. 9. Calculated dependence of (a) the squared frequency of the soft mode R_5 and (b) dynamic matrix elements determining it on the unit cell volume.

elements of the dynamic matrix can be obtained in analytic form. We can separate the contribution ω_C^2 from the Coulomb interaction of ions to frequency so that the remaining term ω_S^2 includes the short-range and long-range dipole–dipole contributions:

$$\omega^2(R_5) = \omega_C^2 + \omega_S^2. \quad (4)$$

Each of these terms can, in turn, be decomposed into two parts corresponding to different elements of the dynamic matrix of the crystal:

$$\omega_C^2 = b_C - f_C, \quad \omega_S^2 = b_S - f_S, \quad (5)$$

$$b = D^{xx}_{F_1-F_1}\left(\mathbf{q} = \frac{\pi}{a}(1, 1, 1)\right), \quad (6)$$

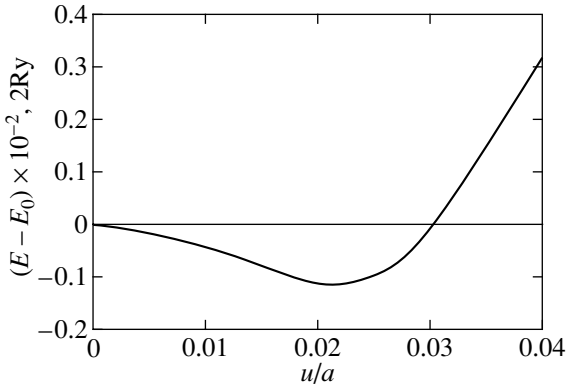

Fig. 10. Dependence of the total energy of a crystal with the doubled unit cell on the displacement of fluorine ions from the equilibrium position of the cubic phase: $E_0 = -2148.9854$; 2Ry is the total energy of the undistorted phase.

$$f = D^{yz}_{F_1-F_2}\left(\mathbf{q} = \frac{\pi}{a}(1, 1, 1)\right), \quad (7)$$

where b and f correspond to longitudinal and transverse force constants of interaction of fluorine ions, respectively. The volume dependence of the quantities appearing in expressions (4) and (5) is also shown in Fig. 9. It can be seen that the Coulomb and short-range contributions to $\omega^2(R_5)$ have opposite signs, and the positive Coulomb contribution exceeds in magnitude the negative short-range contribution under normal pressure, thus ensuring the stability of the cubic phase. As the unit cell volume decreases, both contributions increase in magnitude, but the absolute value of the short-range contribution increases more rapidly than that of the Coulomb contribution, leading to instability of the cubic phase. Figure 9b, presenting the volume dependences of the Coulomb and short-range contributions to the dynamic matrix elements, shows that an increase in the negative short-range contribution to $\omega^2(R_5)$ is mainly associated with the stronger volume dependence of the short-range and dipole–dipole contributions to the diagonal element $D^{xx}_{F_1-F_1}$ ($\mathbf{q} = \pi/a(1, 1, 1)$) of the dynamic matrix. It should be noted that the value of b_S and its dependence on pressure are mainly determined by the contribution from the long-range dipole–dipole interactions.

The structural distortions associated with the condensation of the triply degenerate mode R_5 lead to a rhombohedral distortion of the crystal structure and stabilize the lattice. Figure 10 shows the dependence of the total energy of a crystal with the doubled unit cell on the displacement of fluorine ions from the equilibrium

position of the cubic phase under pressure $P = 6$ GPa:

$$\tilde{u}^x_{F_1} = -\tilde{u}^y_{F_1} = \tilde{u}^y_{F_2} = -\tilde{u}^z_{F_2} = -\tilde{u}^x_{F_3} = \tilde{u}^z_{F_3} = u, \quad (8)$$

$$\tilde{u}^\alpha_{F_i} = \frac{u^\alpha_{F_i}}{2a}\exp(i\mathbf{q}_R\mathbf{r}), \quad (9)$$

where a is the lattice parameter of the cubic phase, $\mathbf{r} = m_1\mathbf{a}_1 + m_2\mathbf{a}_2 + m_3\mathbf{a}_3$ is the translation vector, and $\mathbf{q}_R = \pi/a(1, 1, 1)$. It can be seen that the total energy minimum corresponds to the displacement $u \approx 0.025a$ (0.7 Å) of fluorine ions.

Table 2 contains the values of calculated limiting frequencies of vibrations in the rhombohedral phase in which the coordinates of atoms correspond to the obtained values of the displacement of fluorine ions. The table also gives for comparison the values of frequency at points $\Gamma(\mathbf{q} = (0, 0, 0)$ and $R(\mathbf{q} = \pi/a(1, 1, 1))$ of the undistorted cubic phase as well as the compatibility relations.

After a transition, four lines must be activated in the spectrum (see relation (2)). Two of these lines (A_{1g} and E_g) correspond to the restored soft mode which was split after the transition and, hence, correspond to low frequencies, which must depend considerably on pressure. The three lines observed experimentally above $P = 0.7$ GPa (the frequencies corresponding to these lines are given in Table 2 in parentheses) are in good agreement with this description; the line corresponding to the lowest frequency is noticeably shifted upwards upon an increase in pressure, and the emerging low-frequency wing apparently corresponds to the second mode being restored, whose frequency lies below 150 cm^{-1}. The calculated and experimentally obtained frequencies are in satisfactory agreement. It should be noted that the position of lines correlates well with the frequencies in the Raman spectrum for rhombohedral phases of fluorides of some other trivalent metals [20]. On the whole, we may conclude that the first high-pressure phase is rhombohedral with the space group $R\bar{3}c$, $Z = 2$.

The second point of transition corresponding to a pressure of 3.8 GPa is in good agreement with the transition from the rhombohedral to the orthorhombic (D^{16}_{2h}, $Z = 4$) phase, which was observed earlier in [9]. The strong increase in the number of lines in the Raman spectrum (3) is also in accord with these observations. In [9], a strong diffusion-controlled X-ray scattering was detected above this transition point, which gradually decreased upon an increase in pressure. This correlates well with the emergence of a developed system of domain walls observed through the microscope and with the increase in the domain size under an increase in pressure. The type of this transition (which is predominantly a first-order transition) and the existence of a considerable hysteresis upon a decrease in pressure are also in accord with the results obtained in [9].

Table 2. Compatibility relations and values of vibrational frequencies in the cubic and rhombohedral phases (experimentally measured values of frequencies are given in parentheses)

Cubic phase		Rhombohedral phase	
Frequency, cm^{-1}	Symmetry of vibrations	Symmetry of vibrations	Frequency, cm^{-1}
590	F_{1u}–LO	A_{2u}	557
477	F_{1u}–TO	E_u	442
154	F_{1u}–LO	A_{2u}	210
211	F_{1u}–TO	E_u	164
126	F_{2u}	A_{1u}	148
		E_u	132
542	R_1	A_{2g}	513
341	R_{10}	A_{1u}	327
		E_u	330
445	R_3	E_g	412 (465)
188	R_4	A_{2g}	190
		E_g	198 (260)
65i	R_5	A_{1g}	79 (180)
		E_g	34

6. CONCLUSIONS

Thus, we have carried out experimental studies and numerical calculations of lattice dynamics in a ScF_3 crystal induced by a hydrostatic pressure.

The structural phase transition from the cubic to the rhombohedral phase observed experimentally for the first time under a pressure of 0.7 GPa is in accord with the results of nonempirical calculations of the lattice vibrational spectrum: the calculated spectrum of the crystal under normal pressure contains no imaginary frequencies, which indicates the stability of the structure. However, the vibrational spectrum contains a branch (between points R and M of the Brillouin zone) with anomalously low frequencies. As the unit cell volume decreases (which corresponds to an increase in pressure), the frequencies corresponding to this branch decrease and the lattice becomes unstable at a fairly high pressure. The reason for this decrease in frequency and, hence, in the emergence of lattice instability is the violation of the balance of the Coulomb interactions, on the one hand, and the sum of short-range and dipole–dipole interactions, on the other hand.

The calculated spectrum of the distorted rhombohedral formed as a result of a transition is in good agreement with the experimental spectrum. The experimental Raman spectrum displays the restoration of a soft mode; the frequency of the second expected soft mode apparently lies below the investigated frequency range, and only a wing of this mode is observed.

The pressure and the general type of the second transition from the rhombohedral to the orthorhombic phase investigated by us coincide with those observed earlier [9]; the Raman spectrum of this high-pressure phase is obtained for the first time. The transition is predominantly a first-order transition and is accompanied by strong hysteresis effect. The formation of a complex system of domain walls is apparently responsible for the strong diffuse X-ray scattering (reported in [9]) in this phase. The mechanism of transition to the second high-pressure phase, its structure, and lattice dynamics require further investigations.

ACKNOWLEDGMENTS

The authors are grateful to A.P. Shebanin for his help in experimental measurements.

The work was carried out under financial support from the Russian Foundation for Basic Research (project nos. 00-02-17792 and 00-15-96790) and partly from the INTAS (grant no. 97-10177).

REFERENCES

1. Ph. Daniel, A. Bulou, M. Rousseau, *et al.*, J. Phys.: Condens. Matter **2**, 5663 (1990).
2. K. Rotereau, Ph. Daniel, and J. Y. Gesland, J. Phys. Chem. Solids **59**, 969 (1998).
3. K. Rotereau, Ph. Daniel, A. Desert, and J. Y. Gesland, J. Phys.: Condens. Matter **10**, 1431 (1998).
4. K. S. Aleksandrov, A. T. Anistratov, B. V. Beznosikov, and N. V. Fedoseeva, *Phase Transitions in ABX_3 Crystals* (Nauka, Novosibirsk, 1981).
5. D. Babel and A. Tressaud, in *Inorganic Solid Fluorides* (Academic, London, 1985), p. 77.
6. *Powder Diffraction Data* (International Center on Diffraction Data, 1999), nos. 75-0877, 46-1243, 44-1096, 43-1145, 32-0989, 17-0836.
7. M. M. Aleksandrova, N. A. Bendeliani, V. D. Blank, and T. I. Dyuzheva, Izv. Akad. Nauk SSSR, Neorg. Mater. **26**, 1028 (1990).
8. V. I. Zinenko and N. G. Zamkova, Fiz. Tverd. Tela (St. Petersburg) **42**, 1310 (2000) [Phys. Solid State **42**, 1348 (2000)].
9. N. A. Bendeliani, É. Ya. Atabaeva, and V. M. Agotkov, Izv. Akad. Nauk SSSR, Neorg. Mater. **19**, 816 (1983).
10. K. S. Aleksandov, V. N. Voronov, A. Bulou, *et al.*, in *Abstracts of 6th Japan-CIS Symposium on Ferroelectricity, Noda, Japan, 1998*, p. 152.
11. B. M. Wanklyn, J. Cryst. Growth **5**, 279 (1969).
12. B. M. Wanklyn, J. Mater. Sci. **14**, 1447 (1979).
13. V. A. Timofeeva, *Growth of Crystals from Solutions-Melts* (Nauka, Moscow, 1978).
14. Q. Wang, G. Ripault, and A. Bulou, Phase Transit. **53**, 1 (1995).
15. S. V. Goryainov and I. A. Belitsky, Phys. Chem. Miner. **22**, 443 (1995).
16. R. G. Munro, G. J. Piermarini, S. Block, and W. B. Holzapfel, J. Appl. Phys. **57**, 165 (1985).
17. O. V. Ivanov and E. G. Maksimov, Zh. Éksp. Teor. Fiz. **108**, 1841 (1995) [JETP **81**, 1008 (1995)].
18. V. I. Zinenko, N. G. Zamkova, and S. N. Sofronova, Zh. Éksp. Teor. Fiz. **111**, 1742 (1998) [JETP **87**, 944 (1998)].
19. R. Cowley, Phys. Rev. **134**, 981 (1964).
20. P. Daniel, A. Bulou, M. Rousseau, *et al.*, Phys. Rev. B **42**, 10545 (1990).

Translated by N. Wadhwa